



3 4456 0515422 1

cy. 1

ORNL ISOTOPIC POWER FUELS
QUARTERLY REPORT
FOR PERIOD ENDING JUNE 30, 1972

Eugene Lamb
R. G. Donnelly

OAK RIDGE NATIONAL LABORATORY
CENTRAL RESEARCH LIBRARY
DOCUMENT COLLECTION

LIBRARY LOAN COPY

DO NOT TRANSFER TO ANOTHER PERSON

If you wish someone else to see this
document, send in name with document
and the library will arrange a loan.

UCN-7969
(3-3-67)



OAK RIDGE NATIONAL LABORATORY

OPERATED BY UNION CARBIDE CORPORATION • FOR THE U.S. ATOMIC ENERGY COMMISSION

Printed in the United States of America. Available from
National Technical Information Service
U.S. Department of Commerce
5285 Port Royal Road, Springfield, Virginia 22151
Price: Printed Copy \$3.00; Microfiche \$0.95

This report was prepared as an account of work sponsored by the United States Government. Neither the United States nor the United States Atomic Energy Commission, nor any of their employees, nor any of their contractors, subcontractors, or their employees, makes any warranty, express or implied, or assumes any legal liability or responsibility for the accuracy, completeness or usefulness of any information, apparatus, product or process disclosed, or represents that its use would not infringe privately owned rights.

ORNL-4814
UC-33 -- Propulsion Systems
and Energy Conversion

Contract No. W-7405-eng-26

ISOTOPES DEVELOPMENT CENTER

ORNL ISOTOPIC POWER FUELS QUARTERLY REPORT
FOR PERIOD ENDING JUNE 30, 1972

Eugene Lamb

Isotopes Division

R. G. Donnelly

Metals and Ceramics Division

AUGUST 1972

OAK RIDGE NATIONAL LABORATORY
Oak Ridge, Tennessee 37830
operated by
UNION CARBIDE CORPORATION
for the
U.S. ATOMIC ENERGY COMMISSION

LOCKHEED MARTIN ENERGY RESEARCH LIBRARIES



3 4456 0515422 1

CONTENTS

	<u>Page</u>
SUMMARY	1
CURIUM-244 FUEL DEVELOPMENT	2
Curium-244 Oxide Fuel Development and Properties	2
Heat Capacity of $^{244}\text{Cm}_2\text{O}_3$	2
Kilowatt Heat Source Examination	2
Vented Capsule Fuel Form Study	2
Preparation of Sized $^{244}\text{Cm}_2\text{O}_3$ Particles	2
Helium Release from Cermets	3
Cermet Test Program	3
Metallography of Curium Source Test Fuel	4
Recovery of Curium-244 from Fuel Reprocessing Waste	4
Curium Source Neutron Dose Measurement	4
Impact Testing of Heat Source Materials	4
Velocity Measurement System	4
Impact Gun Testing	4
CLADDING MATERIALS PROGRAM	9
Characterization of Pt-Rh-W Alloys	9
Characterization of Iridium	16
PHYSICAL METALLURGY OF REFRACTORY ALLOYS	17
Effect of Oxygen Contamination on the Mechanical Properties of Molybdenum-Base Alloys	17
Effect of Carbon Monoxide Contamination on the Mechanical Properties of Molybdenum-Base Alloys	19
MATERIALS COMPATIBILITY TESTING FOR THE LASL-DART PROJECT	20
REFERENCES	23

LIST OF FIGURES

Fig. 1. Calibration Curve for Impact Testing Gun	7
Fig. 2. Firing Characteristics of Impact Testing Gun	8

LIST OF TABLES

	<u>Page</u>
Table 1. Repeatability of Impact Gun	6
Table 2. Data on Firing of Impact Gun with Unheated Sabots	6
Table 3. Correlation Between Nondestructive Testing Inspection and Room-Temperature Tensile Properties of Pt-26% Rh-8% W	9
Table 4. The Effect of Annealing Temperature and Rolling Direction on the Room-Temperature Tensile Properties of 0.030-in.-thick Pt-26% Rh-8% W Sheet	10
Table 5. Results of Annealing 1 Hr at Various Temperatures on the Cup Height Obtained on 0.030-in.-thick Pt-26% Rh- 8% W Alloy Sheet in a Modified Olsen Cup Test	10
Table 6. Bend Test Results of 0.030-in.-thick Platinum-Rhodium-Tungsten Alloy Sheet	11
Table 7. Tensile Properties of 0.030 × 12 × 12-in. Sheet of Pt-26% Rh-8% W	12
Table 8. The Effect of Strain Rate on the Tensile Properties of Pt-26% Rh-8% W Sheet at 1316°C	12
Table 9. Tensile Properties of 0.030-in.-thick Pt-30% Rh-8% W	13
Table 10. Results of 2T Bend Test Showing Effect of Surface Treatment of 0.030-in.-thick Pt-30% Rh-8% W Alloy Sheet Heat Treated 1 Hr at 990°C in Vacuum	14
Table 11. Effect of Heat Treatment on Bend Behavior of Pt-26% Rh-8% W Alloy Samples After Removal of 0.0045 in. from the Tension Side of Sample	15
Table 12. Results of 2T Bend Test Showing Effect of Heat Treatment of Electron-Beam Welds in 0.030-in.-thick Pt-26% Rh-8% W Alloy Sheet	15
Table 13. Tensile Properties of Commercial Iridium Recrystallized 1 Hr at 1500°C	16
Table 14. Tensile Properties of Commercial Iridium Annealed 5 Min at 2000°C after Recrystallization for 1 Hr at 1500°C	17
Table 15. Tensile Properties of 20-mil-thick TZM Sheet Specimens Doped with Oxygen at 1×10^{-5} Torr at 1000°C and Tested at Various Temperatures	18

	<u>Page</u>
Table 16. Tensile Properties of 20-mil-thick TZM Sheet Specimens Contaminated with CO at 1×10^{-5} Torr and 1000°C and Tested at Various Temperatures	19
Table 17. Summary of 1400°C Compatibility Test Data for LASL-DART Project	21
Table 18. Summary of 1500°C Compatibility Test Data for LASL-DART Project	22
Table 19. Summary of Weight Change Data on Compatibility Couples	23

ORNL ISOTOPIC POWER FUELS QUARTERLY REPORT
FOR PERIOD ENDING JUNE 30, 1972

Eugene Lamb and R. G. Donnelly

SUMMARY

Preparation for cutting samples from the tungsten fuel block of the Kilowatt Heat Source for metallographic examination are underway. Installation of test facilities for studies of helium release and identification of other volatile species released from vented fuel forms in a high-temperature, high-vacuum environment container is 50% completed.

A large batch of Gd_2O_3 microparticles was prepared for use in making an experimental Ir- Gd_2O_3 cermet. Tests to determine the effect of alpha damage on the helium permeation of metals were initiated. Curium oxide powder was placed in contact with an aluminum foil thinner than the range of alpha particles in the aluminum. No detectable amount of helium permeation was observed after 4 weeks of alpha irradiation. The x-ray diffraction study of the fuel sample from the Curium Source Test showed that the fuel was $^{244}Cm_2O_3$, but due to high radiation levels from the ^{244}Cm no conclusion as to impurities or concentration could be made. The preliminary design of a process for separating curium from fission products has been completed. The process consists mainly of removing the lanthanide-actinide fraction by solvent extraction in a differential extraction system.

The laser beam velocity measurement system has been installed and tested with the impact gun. Repeatability of the impact gun is excellent. The impact gun has been calibrated so that specimens can be impacted at any desired velocity.

Variable mechanical properties obtained on Pt-Rh-W sheet were traced to tungsten segregation and/or surface defects. Inspection and processing changes have been instituted to overcome these problems. Annealing temperatures have been determined for optimum formability, and mechanical properties are shown to be nondirectional in finished sheet. Property improvement is indicated in material with the rhodium content increased from 26 to 30% while the tungsten content is maintained at 8%.

The mechanical properties of iridium sheet were determined as a function of temperature. No sharp ductile-to-brittle

transition temperature was observed. The effects of a simulated reentry heat pulse on the mechanical properties of iridium were also determined.

TZM was found to be incompatible with low-pressure oxygen at 1000°C. Reduced ductility is also observed in TZM exposed to CO at 1000°C. Compatibility testing of a wide variety of nonfuel materials couples has been completed and examined in support of the DART program.

CURIUM-244 FUEL DEVELOPMENT

(Division of Space Nuclear Systems Program 04 30 05 03)

Curium-244 Oxide Fuel Development and Properties

Heat Capacity of $^{244}\text{Cm}_2\text{O}_3$

Various tools necessary to handle the $^{244}\text{Cm}_2\text{O}_3$ heat capacity sample were made, and a trial run for loading the sample into the experimental apparatus was successfully carried out.

Kilowatt Heat Source Examination

Preparation for the metallurgical examination of samples cut from the tungsten fuel block was begun. The first step, involving the opening of the container in which the fuel block was stored, was initiated. The second step will be the removal of the major quantity of $^{244}\text{Cm}_2\text{O}_3$ from the fuel channels. The third step will include sectioning of the fuel block and metallographic inspection of selected specimens in HRLEL.

Vented Capsule Fuel Form Study

Installation of a high-temperature, high-vacuum furnace for testing fuel forms in vented capsules is 50% completed. The test is to simulate and study the effects of space-like conditions on the fuel form of a prototype vented capsule. The helium release characteristics of the fuel form will be determined, and the residual atmosphere in the furnace and the possible vapor species from the fuel form will be measured. Following the exposures at temperature, the specimens will be sectioned and examined for compatibility effects. The test facility enclosed in a shielded alpha glove-manipulator cell consists of a Brew-type furnace, a turbomolecular pump, and a quadrupole mass spectrometer for analyses of gaseous and vapor species.

Preparation of Sized $^{244}\text{Cm}_2\text{O}_3$ Particles

A large batch of Gd_2O_3 microparticles was prepared for use in making an experimental Ir- Gd_2O_3 cermet. The preparation of this material used the available resin. More of the same brand and type was obtained; however,

it behaves differently and leads to the frequent fracturing of particles. The two resins which had been previously used successfully were Rexyn 102H and IRC-72. In a recently purchased batch of Rexyn 102H the particles differed appreciably from the old resin in physical form and in ion-exchange capacity. Tests with the resin were abandoned. A new batch of IRC-72 was the same in appearance and in nominal capacity; however, many of the beads were observed to break in both the loading and the carbonization steps. This difficulty had not been encountered in earlier tests with certain exceptions. The beads of a batch of very highly bonded material had been badly broken and beads which had been initially in the NH_4^+ form tended to break during carbonization. It also had been found that the presence of oxygen during carbonization caused all types of beads to break.

The breaking of beads during loading was eliminated by a change in procedure to eliminate agitation during loading. A loading apparatus was developed which operates on the principle of the coffee percolator in which the solution percolates through a bed of the resin.

Work continued on the adaptation of the resin process to hot-cell operation by defining the heating cycle required to minimize particle breakage and optimize sintering. Equipment for hot-cell preparation of $^{244}\text{Cm}_2\text{O}_3$ particles has been fabricated.

Helium Release from Cermets

Tests to determine the effect of alpha damage on the helium permeation of metals were initiated.¹ Curium oxide powder was placed in contact with an aluminum foil of thickness less than the range of alpha particles in the aluminum. A pressure of helium of 17 lb/in.² was put on the aluminum foil while the opposite side of the foil was connected to a mass spectrometer to determine helium permeation of the foil. After four weeks of alpha irradiation, no detectable amount of helium permeation was observed. An annealed platinum foil, 8.3 μm thick, is being tested, but no results are available.

Cermet Test Program

Strength deterioration and reduced helium permeability of $^{244}\text{Cm}_2\text{O}_3$ -bearing cermets upon aging are of particular concern to the development of an isotopic power fuel form. We are investigating these effects in Mo-ThO₂ compacts.¹

Aging of Mo-ThO₂ specimens for 1000 hr at 1200 and 1500°C and $<10^{-5}$ torr was completed. All aged specimens appeared to be in excellent condition. Specimens hot-pressed at 1200°C showed a slight increase in density from a corresponding reduction in physical dimensions. The aging treatments produce little, if any, significant change in specimens hot-pressed at 1450 and 1700°C. Due to a change in programmatic priorities no further evaluation of these specimens is planned.

Metallography of Curium Source Test Fuel

The x-ray diffraction study of the fuel sample from the Curium Source Test was terminated. The study showed that the fuel was $^{244}\text{Cm}_2\text{O}_3$. Due to high radiation levels from the ^{244}Cm no conclusion as to impurities or concentration could be made.

Recovery of Curium-244 from Fuel Reprocessing Waste

The preliminary design of a process for separating curium from fission products has been completed. The process consists essentially of the removal of a lanthanide-actinide fraction from the mixed fission products by solvent extraction using the differential extraction process. This is followed by the separation of the curium from the lanthanides and other actinides by a chromatographic ion-exchange process. The process was designed to minimize capital costs and to avoid any appreciable increase in the volume of solid wastes.

Curium Source Neutron Dose Measurement

The water shielding tank to be used in the curium neutron dose measurement experiment was completed.

Impact Testing of Heat Source Materials

Velocity Measurement System

The laser beam velocity measurement system was installed and tested with the impact gun. Some minor problems were experienced with the system being too sensitive to shock waves generated by the impact of the sabot on the wall of the catcher box. The eye of the photosensor was so small that, if the laser beam deviated only a small amount due to vibrations, the system would generate enough of a pulse to start the electronic timer. The original photosensors were replaced with ones having a larger eye which would allow the laser beam to vibrate on the eye and trigger the timer only upon total eclipse of the beam. This change eliminated the premature triggering of the timer.

Impact Gun Testing

The toggle brackets for the sabot heater electrical connections were installed in the impact gun gas chamber. Tests of the heater system indicated that 1000°C can be attained.

The impact gun sabot gripper was energized with the heater at the maximum temperature to test the system at temperature. Gas could be heard escaping around the sabot during the test, and only 150-psig gas pressure could be maintained on the system with the gas regulator wide open. The gun was disassembled, and the gripper was dimensionally inspected. A

0.006-in. permanent distortion was found in the center of the gripper indicating that the gripper and gun had expanded more than had been anticipated. A new sabot heater and gripper were designed to provide proper clearances for impact testing of pellets at 700°C. The gripper was energized with the heater at 750°C and the pressure was adjusted to 250 psig with no apparent leakage of gas.

To test the repeatability of the impact gun, five aluminum sabots were test fired. The projectile used in this test was a 1-in.-diam steel ball. Table 1 shows the excellent repeatability of the impact gun.

In order to impact specimens at any desired velocity within the range of the gun, a calibration of the gun relating firing pressure, mass, and velocity is being made. Table 2 lists the data collected to date on the firing of the impact gun using unheated sabots.

Figure 1 shows a plot of firing pressure versus kinetic energy $\times 32 \times 10^{-3}$. (To calculate kinetic energy in ft-lb, "M" must be in slugs, but direct substitution of the weight of the sabot and specimen is more convenient; thus the term kinetic energy $\times 32$.) By assuming that the equation of the straight line shown in Fig. 1 has the form:

$$P = S(MV^2/2) + b \quad (1)$$

where

P = firing pressure, psig

M = sabot and specimen weight, lb

V = specimen velocity, ft/sec

S = slope of line, (lb of force sec²)/(lb of mass ft² in.²)

b = intercept of line, psig

then by the classical slope-intercept method, the equation of the impact testing gun was found to be

$$P = (1.464 \times 10^{-3})MV^2 \quad (2)$$

Equation (2) has been found to be very reliable in setting the firing pressure for a desired velocity, given the weight of the sabot and specimen. A nomograph (Fig. 2) was constructed using Eq. (2) written in the form

$$\text{Log } P = \text{Log } M + 2 \text{ Log } V - 2.83446 \quad (3)$$

The data used to derive Eq. (2) were from tests in which the impacted specimen and sabot were not heated. Further tests will be made to determine if the equation holds true for impacts with heated specimens.

A 3/4-in.-diam gadolinium sesquioxide (Gd₂O₃) sphere was heated to 750°C and impacted on a granite block. The sabot and specimen weight was 532.8 g, and the sabot was fired at 125 psig. A high-speed movie was

Table 1. Repeatability of Impact Gun

Firing Pressure (psig)	Sabot and Sample Weight (lb)	Interval Time ^a (sec)	Velocity (ft/sec)
140	1.498	0.00394	253.8
140	1.498	0.00395	253.2
250	1.498	0.00297	336.7
250	1.498	0.00296	337.8
200	1.498	0.00331	302.1

^aInterval time measured over a distance of 1 ft.

Table 2. Data on Firing of Impact Gun with Unheated Sabots

Pressure (psig)	Weight (lb)	Time (msec)	Velocity (ft/sec)	Kinetic Energy $[(1/2 MV^2) \times 32 \times 10^{-3}]$	Velocity Measuring System ^a
100	1.542	4.83	207.0	33.0	1
100	1.542	4.82	207.0	33.0	1
125	1.520	4.32	231.5	40.7	3
125	1.520	4.27	234.2	41.7	3
140	1.498	3.94	253.8	48.2	1
140	1.498	3.95	253.2	48.0	1
140	1.571	4.04	247.5	48.1	1
140	1.563	4.03	248.1	48.1	1
180	2.000	3.99	250.6	62.8	2
180	2.000	4.01	249.4	62.2	2
180	2.000	4.04	247.5	61.3	2
180	1.219	3.10	322.5	63.4	2
190	1.520	—	291.0	64.4	4
190	1.520	3.49	286.5	62.4	3
200	1.498	3.31	302.1	68.3	1
200	1.504	3.50	285.7	61.4	1
250	1.498	2.97	336.7	84.9	1
250	1.498	2.96	337.8	85.4	1
250	1.672	3.13	319.5	85.3	1
125 ^b	1.174	—	263.8	40.8	4

^aVelocity Measuring System Code: 1 - ORNL laser timing system; 2 - Process Equipment Company timing system; 3 - ORNL photoelectric timing system; 4 - High-speed movies.

^bData not shown in Fig. 1.

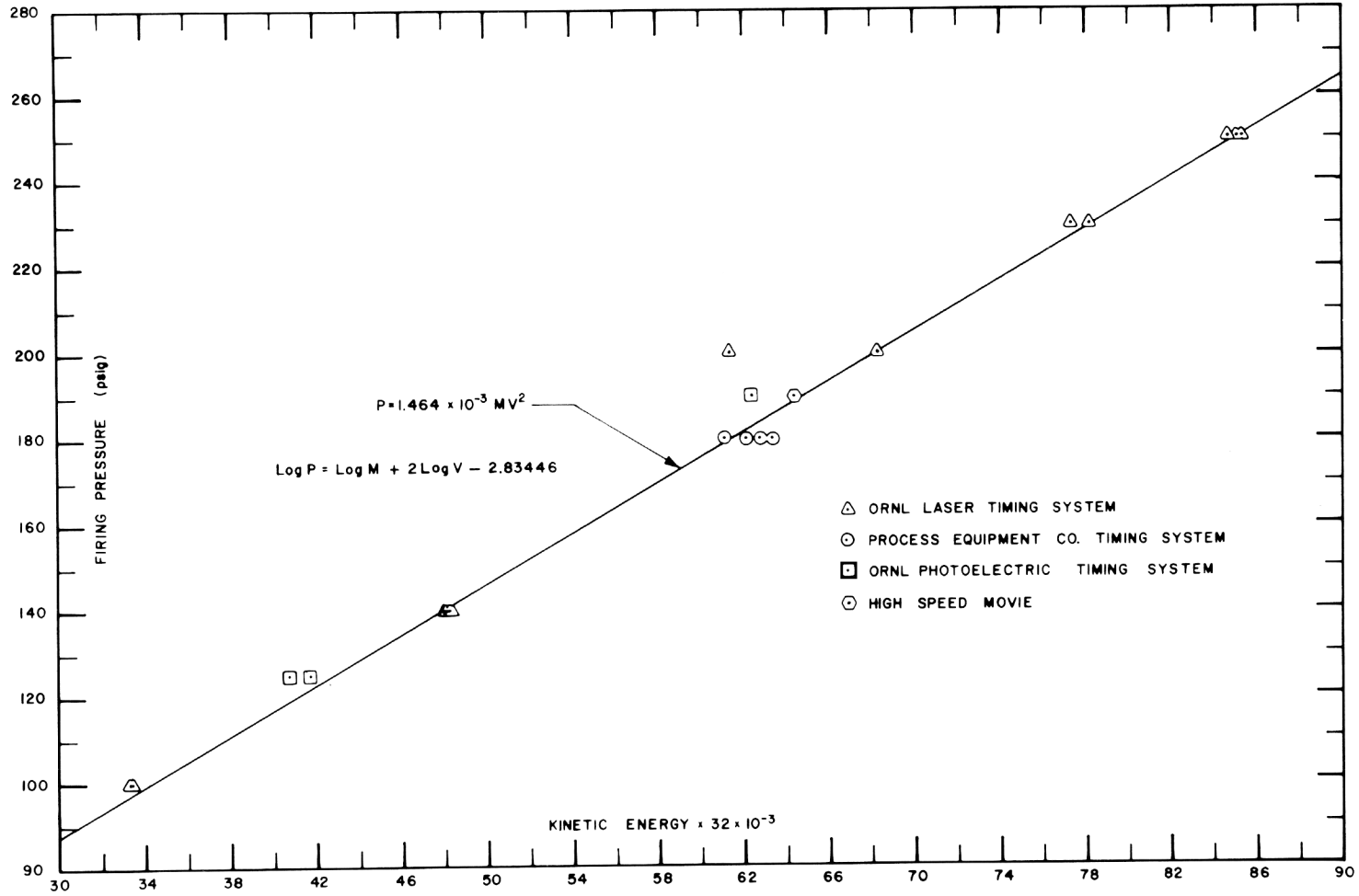


Fig. 1. Calibration Curve for Impact Testing Gun.

taken of the impact. The impact velocity predicted from the gun equation [Eq. (2)] was 269.7 ft/sec, and the velocity obtained from analyzing the high-speed movie was 263.8 ft/sec. Comparison of this movie with others taken of unheated Gd_2O_3 spheres being impacted showed no visible difference in the breakup of the spheres.

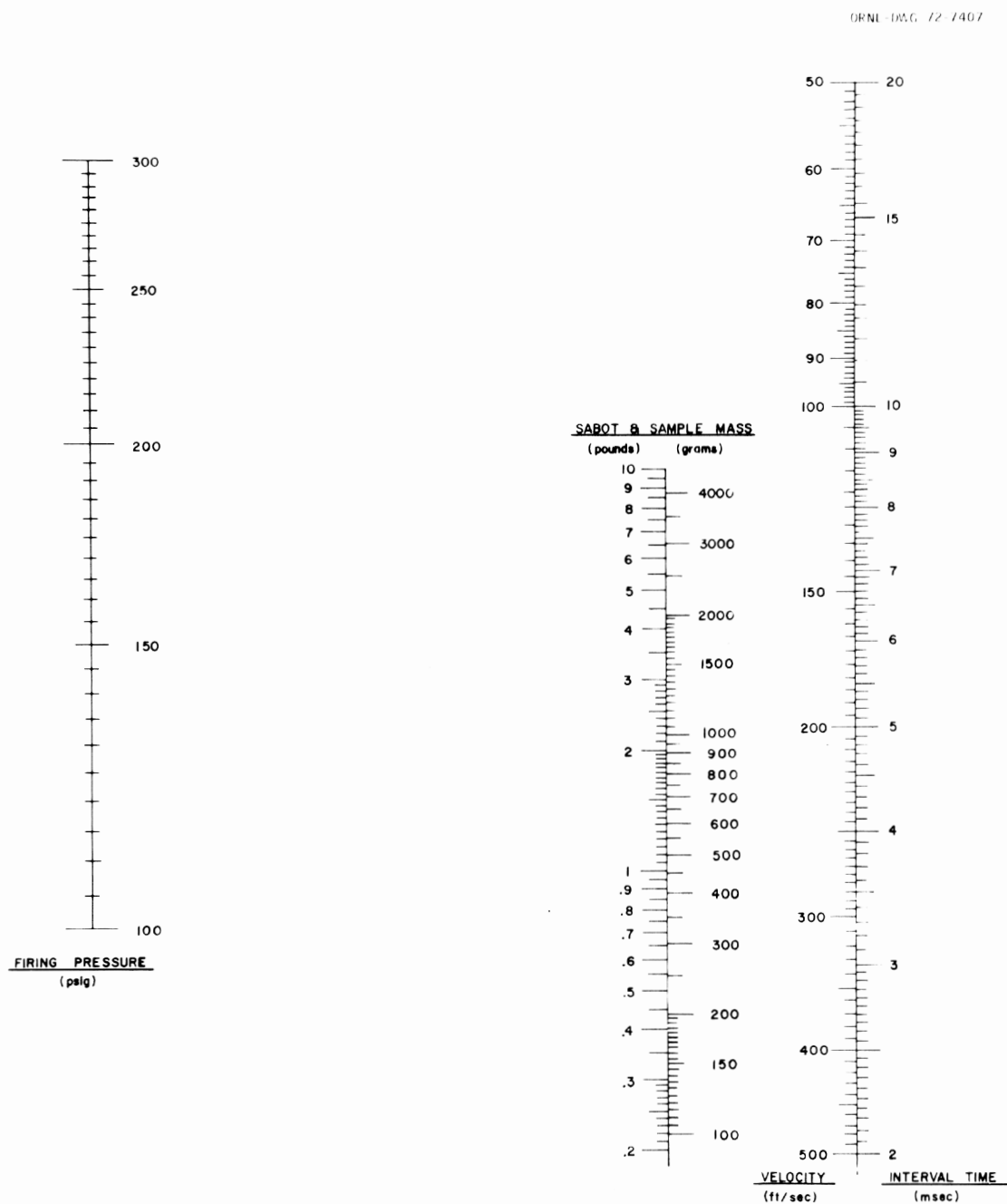


Fig. 2. Firing Characteristics of Impact Testing Gun.

CLADDING MATERIALS PROGRAM

(Division of Space Nuclear Systems Program 04 30 05 04)

Characterization of Pt-Rh-W Alloys

J. H. Erwin and H. Inouye
Metals and Ceramics Division

Previously we reported that the 0.030 × 8-1/2 × 11-in. sheet prepared from a 4-lb ingot (Heat Pt-1D, nominal composition Pt-26% Rh-8% W) was shown by eddy current inspection to contain isolated areas of tungsten segregation.¹ Metallographic examination of the cross section of an area indicating maximum segregation showed up as a 0.0005-in.-wide tungsten stringer extending the length of the specimen. To further evaluate the nondestructive results, tensile specimens were blanked from the sheet so that the indicated areas of segregation were in the gage section. Table 3 shows that the strength and ductility of specimens showing segregation were generally lower than the homogeneous specimens. The lack of a better correlation is attributed to missing the segregated areas which were as small as 1/16 in. in diameter. We conclude from these results that the eddy current method is a reliable quality-control technique for detecting tungsten segregation.

The effect of annealing temperature and the directional properties of the homogeneous portions of sheet Pt-1D are shown in Table 4. The specimens show the characteristic decrease in strength and increase in ductility with increasing annealing temperature. No significant directional properties are evident. This may be due to the cross rolling during warm reduction at 1000°C.

Table 3. Correlation Between Nondestructive Testing Inspection and Room-Temperature Tensile Properties^a of Pt-26% Rh-8% W (Heat Pt-1D)

Eddy Current Reading ^b	Ultimate Tensile Strength (psi)	Yield Strength (psi)	Elongation (%)
<1	88,800	48,700	10.0
<1	92,200	48,000	11.0
164	91,400	48,000	10.8
214	84,400	49,100	8.7
396	70,000	47,500	5.0
445	90,300	49,500	10.1
488-538	83,700	48,800	8.3

^a0.030-in.-thick sheet, annealed 1 hr at 1200°C, tested at 0.05 in./in./min.

^bThe severity of tungsten segregation is thought to increase with these numbers. Values of <1 are considered to be homogeneous.

Table 4. The Effect of Annealing Temperature and Rolling Direction on the Room-Temperature Tensile Properties of 0.030-in.-thick Pt-26% Rh-8% W (Heat 1D) Sheet^a

Heat Treatment	Ultimate Tensile Strength (psi)	Yield Strength (psi)	Elongation (%)
<u>Parallel to Rolling Direction</u>			
Cold Rolled 21%	182,100	154,000	2.0
Annealed 1 hr at 1000°C	153,200	122,500	7.3
Annealed 1 hr at 1100°C	97,100	53,800	10.5
Annealed 1 hr at 1200°C	92,200	48,000	11.0
Annealed 1 hr at 1300°C	83,700	43,800	10.4
<u>Transverse to Rolling Direction</u>			
Cold Rolled 21%	186,500	149,000	2.9
Annealed 1 hr at 1000°C	157,700	123,800	11.4
Annealed 1 hr at 1100°C	100,000	55,300	11.5
Annealed 1 hr at 1200°C	92,500	48,700	11.4
Annealed 1 hr at 1300°C	81,200	45,200	9.4

^aStrain rate is 0.05 in./in./min.

Using hydrogen-annealed powder instead of arc-melted and crushed tungsten and a modified melting procedure,¹ an additional 4-lb ingot of Pt-26% Rh-8% W (Heat Pt-1ER) was cast and successfully rolled to 0.030-in.-thick sheet using the same fabrication procedures previously used. Eddy current inspection of this sheet showed no indication of tungsten segregation. To date the formability of this sheet, as determined by a modified Olsen cup test, is shown in Table 5. The results are compared with blanks taken from the homogeneous areas of Heat Pt-1D. The cup height as a function of the heat treatment shows no appreciable difference between the two heats and a peak in the formability of specimens annealed between 990 and 1000°C. According to our previous studies, a 1-hr anneal at this temperature is just at or below the recrystallization temperature.

Table 5. Results of Annealing 1 Hr at Various Temperatures on the Cup Height Obtained on 0.030-in.-thick Pt-26% Rh-8% W Alloy Sheet in a Modified Olsen Cup Test

Heat Treatment Temperature (°C)	Cup Height (in.)	
	Pt-1D ^a	Pt-1ER ^b
900	0.305	0.287
950	0.307	0.309
990	Not tested	0.467
1000	0.464	0.427
1050	0.278	0.257
1100	0.270	0.387
1200	0.241	0.257
1300	0.264	0.261

^aSheet contained segregated areas of tungsten, but not in areas of sample blanks.

^bSheet showed no segregation.

Bend test results of similarly heat-treated samples from the two sheets are summarized in Table 6. The bend test is the standard 2T test described in *Evaluation Test Methods for Refractory Metal Sheet Specimens*, MAB-176M (1961). In this respect, these data verify the 1000 to 1100°C temperature range indicated by the tensile and cup tests as optimum heat treatment for the 21% cold-rolled alloy. The calculated elongation and bend strength are 25 to 50% higher than the values obtained from tensile tests. This is perhaps due to differences in sample geometry and calculation methods. Duplicate samples for a given heat treatment showed occasional wide differences in the bend angle to failure. Examination of the fractures reveal grain boundary separation in the less ductile samples. We associated the grain boundary fracture with tungsten segregation from previous experience with the Pt-1D sheet; however, examination of samples by metallography has not revealed any differences in grain boundaries of the samples.

The tensile properties of Pt-26% Rh-8% W (heat Pt-1ER) specimens taken from an 0.030 × 12 × 12-in. sheet are shown in Table 7. These data show consistent and nondirectional properties for a given heat treatment. The ductility increases uniformly with temperature from approximately 11% at room temperature to approximately 50% at 1316°C. On the other hand, the reduction in area is seen to increase abruptly from approximately 6% at room temperature to 100% at and above 760°C. Table 8 shows that the calculated impact capabilities at 1316°C of the alloy [defined as 0.5(UTS + YS) × fracture strain] increase somewhat with the strain rate by virtue

Table 6. Bend Test^a Results of 0.030-in.-thick Platinum-Rhodium-Tungsten Alloy Sheet

Heat Treatment ^b (°C)	Maximum Bend Angle (deg)			Elongation (%)			Bend Strength (ksi)		
	Pt-1D ^c	Pt-1ER ^d	Pt-4A ^e	Pt-1D ^c	Pt-1ER ^d	Pt-4A ^e	Pt-1D ^c	Pt-1ER ^d	Pt-4A ^e
<u>Transverse Samples Bent Parallel to Cold-Rolling Direction</u>									
900	61	53	55	12.3	11.6	11.7	309	332	329
950	86	55	x	17.2	12.0	x	286	304	x
990	x	99	108	x	19.0	>20	196	209	214
1000	65	x	x	13.4	x	x	258	x	x
1050	80	60	x	16.4	12.8	x	166	170	x
1100	81	50	108	16.5	10.7	>20	153	145	152
1200	37	x	x	8.2	x	x	131	x	x
1300	35	42	87	8.1	9.5	18.0	118	115	136
<u>Longitudinal Samples Bent Transverse to the Cold-Rolling Direction</u>									
900	70	46	x	13.9	10.0	x	292	313	x
950	86	64	x	19.1	13.3	x	269	300	x
990	x	64	x	x	13.3	x	x	193	x
1000	88	x	x	17.2	x	x	234	x	x
1050	70	52	x	14.6	11.2	x	153	167	x
1100	89	50	x	17.4	10.6	x	141	143	x
1200	45	45	x	9.7	9.7	x	125	129	x
1300	40	46	x	8.7	9.8	x	112	118	x

^a2T bend test was made at a rate of 0.2 in./min.

x = no sample.

^bOne-hour vacuum.

^cPt-26% Rh-8% W sheet showing segregation of tungsten.

^dPt-26% Rh-8% W sheet with no segregation indicated.

^ePt-30% Rh-8% W sheet.

Table 7. Tensile Properties of 0.030 × 12 × 12-in. Sheet of Pt-26% Rh-8% W (Heat Pt-1ER)^a

1-Hr Heat Treatment (°C)	Test Temperature (°C)	Ultimate Tensile Strength (psi)	Yield ^b Strength (psi)	Elongation (%)	Reduction in Area (%)
<u>Longitudinal to Rolling Direction</u>					
1000	Room	152,000	103,000	11.5	11.9
1100	Room	104,800	53,100	13.5	6.1
1200	Room	92,100	47,300	11.5	7.5
1300	Room	80,700	40,400	11.1	5.7
1200	760	74,400	28,700	27.8	~100
1200	1093	38,400	18,900	30.8	~100
1200	1316	17,000	14,900	52.0	~100
<u>Transverse to Rolling Direction</u>					
1000	Room	150,300	109,700	13.8	15.3
1100	Room	101,000	55,000	13.3	5.3
1200	Room	91,600	49,400	11.3	7.2
1300	Room	74,800	42,000	9.3	6.0

^aCold rolled 21% before annealing (strain rate 0.05 in./in./min.).

^b0.2% offset yield strength.

Table 8. The Effect of Strain Rate on the Tensile Properties of Pt-26% Rh-8% W Sheet at 1316°C

Strain Rate (in./in./min)	Ultimate Tensile Strength (psi)	Yield ^b Strength (psi)	Elongation (%)	Impact Values ^c (in.-lb/in. ³)
0.05	17,000	14,900	52.0	16,600
0.10	20,100	17,600	56.5	21,200
0.20	20,700	16,900	47.0	17,700

^a0.030-in.-thick sheet of Pt-1ER annealed 1 hr at 1200°C.

^b0.2% offset yield strength.

^c0.5(UTS + YS) × fracture strain.

of corresponding increases in the ultimate tensile and yield strength. The impact values for T-111 and iridium are 11,000 and 7,400 in.-lb/in.³, respectively. The superior impact values of the platinum alloy arise from the fact that the yield strength is about 86% of the ultimate strength and that the fracture ductilities are also higher than T-111 or iridium.

To determine the effect of the rhodium content in Pt-Rh-W alloys, we increased the rhodium content from the previous 26% to 30% at the 8% W level. One small ingot (heat Pt-4A) was fabricated into sheet in a manner similar to previous procedure with excellent results. An Olsen cup test

on a blank heat treated for 1 hr at 990°C in vacuum produced a full 7/8-in.-diam hemisphere with only two small surface cracks. This is in contrast with failure of the Pt-26% Rh-8% W alloy (Pt-1ER) blank at a cup height of only 0.467 in. Results of the bend tests on this alloy are also given in Table 6. Samples heat treated at both 990 and 1100°C withstood a 90° 2T bend test.

The tensile properties of heat Pt-4A are shown in Table 9. At room temperature this alloy is stronger and more ductile than Pt-26% Rh-8% W; however, at 1093 and 1316°C a significant amount of scatter was observed. Because the specimens showing poor tensile properties were taken from the same side of the rolled sheet, it is suspected that contamination or segregation has occurred.

Table 9. Tensile Properties of 0.030-in.-thick Pt-30% Rh-8% W (Heat Pt-4A)^a

Test Temperature (°C)	Ultimate Tensile Strength (psi)	0.2% Offset Yield Strength (psi)	Elongation (%)	Reduction in Area (%)
<u>Longitudinal to Rolling Direction</u>				
Room	115,000	53,200	17.8	9.1
1093 ^b	38,000	20,500	16.8	13.4
1316	19,800	16,500	46.8	57
<u>Transverse to Rolling Direction</u>				
Room	108,200	50,800	18.8	9.1
760	75,100	30,200	30.2	35.1
1093 ^b	35,700	19,500	18.3	35.4
1316 ^b	15,500	15,000	28.0	11.9

^aSpecimens annealed 1 hr at 1200°C, tested at 0.05 in./in./min.

^bSpecimens showed numerous cracks in gage length after testing.

To assess the effect of observed subsurface voids on erratic mechanical properties, the surfaces of six adjacent bend test specimens from a 0.030-in.-thick Pt-30% Rh-8% W alloy sheet (Pt-4B) were ground, heat treated, and given a 2T bend. The results are given in Table 10. No appreciable difference appears between the as-rolled samples and those polished to remove about 0.0005 in. from the surface. However, both samples that were ground to remove 0.003 in. followed by polishing the surface withstood the 2T bend test without failure. To further verify the effect of the voids, three sets of three samples each were taken from a Pt-26% Rh-8% W alloy sheet (Pt-1ER) that had previously shown inconsistent bend test results. The samples were filed and polished to remove about 0.0045 in. from the surface followed by heat treatment in air at 1000°C and in vacuum at 1000 and 1100°C. Data from these samples (Table 11) show no difference in the ductility of the vacuum heat-treated

samples. However, samples oxidized 4 hr in air at 1000°C (approximates the final hot-rolling temperature and heating time) failed at a 50° bend angle and an elongation of 10.5%.

An examination indicates that the depth of the voids reaches a maximum after a short exposure at a given temperature and that their size and perhaps number also increase with time. Pt-30% Rh-8% W (Pt-4B) and Pt-26% Rh-8% W (Pt-1ER) alloy samples oxidized 4 and 8 hr contain voids with a maximum depth of about 1 mil and an average depth of 1/4 to 1/2 mil. Pt-30% Rh-8% W (Pt-4B) samples oxidized 19 hr at 1200°C contain voids with a maximum depth of about 3 mils and an average depth of 1 mil.

To assess the weldability of 0.030-in.-thick sheet, test specimens containing transverse electron-beam welds were filed to reduce the weld bead to the thickness of the original sheet and were given a 2T bend test. Data shown in Table 12 indicate bend angle at failure, elongation, and bend strength about 75% of that expected for similar unwelded samples. Failure usually occurred in the welds.

Table 10. Results of 2T Bend Test^a Showing Effect of Surface Treatment of 0.030-in.-thick Pt-30% Rh-8% W Alloy Sheet Heat Treated 1 Hr at 990°C in Vacuum

Sample Number	Maximum Bend Angle (degrees)	Elongation (%)	Bend Strength (ksi)
<u>As Rolled</u>			
Pt-4B-2	75	15.0	255
Pt-4B-5	50	10.6	282
<u>Polished</u>			
Pt-4B-1	70	14.3	266
Pt-4B-4	74	15.0	279
<u>0.003 in. Removed and Polished</u>			
Pt-4B-3	110	>20	275
Pt-4B-6	110	>20	272

^a2T bend test was made at 0.2 in./min.

Table 11. Effect of Heat Treatment on Bend^a Behavior of Pt-26% Rh-8% W Alloy Samples After Removal of 0.0045 in. from the Tension Side of Sample

Sample Number	Maximum Bend Angle (degrees)	Elongation (%)	Bend Strength (ksi)
<u>4 Hr, 1000°C, Air</u>			
Pt-1ER-17	50	10.6	202
Pt-1ER-18	50	10.5	228
Pt-1ER-22	50	10.6	212
<u>1 Hr, 1000°C, Vacuum</u>			
Pt-1ER-19	115 ^b	>20	170
Pt-1ER-20	115 ^b	>20	203
Pt-1ER-21	115 ^b	>20	187
<u>1 Hr, 1100°C, Vacuum</u>			
Pt-1ER-23	115 ^b	>20	150
Pt-1ER-24	115 ^b	>20	151
Pt-1ER-25	115 ^b	>20	149

^a2T bend test was made at 0.2 in./min.

^bFull bend.

Table 12. Results of 2T Bend Test^a Showing Effect of Heat Treatment of Electron-Beam Welds in 0.030-in.-thick Pt-26% Rh-8% W Alloy Sheet (Heat Pt-1ER)

Sample Number	Maximum Bend Angle (degrees)	Elongation (%)	Bend Strength (ksi)
<u>1 Hr at 990°C Vacuum</u>			
W-1	30	7.3	139
W-2	35	8.2	164
<u>1 Hr at 1200°C Vacuum</u>			
W-3	55	12.2	137
W-4 ^b	102	>20	141

^a2T bend test was made at a rate of 0.2 in./min.

^bBend in heat-affected zone.

Characterization of Iridium

C. T. Liu
Metals and Ceramics Division

Recent thermal analysis at General Electric indicates that the minimum impact temperature for the MHW heat source is about 593°C.² Since this temperature is close to the ductile-to-brittle transition temperature (DBTT) of iridium which was reported to be ~500°C,³ it is important to determine the DBTT of iridium and how it varies with thermal treatments such as might be experienced during fabrication, operation, or reentry.

For this purpose, iridium sheet specimens recrystallized 1 hr at 1500°C were tested at various temperatures. The tensile data are listed in Table 13 and show:

1. The room-temperature yield strength of recrystallized iridium is only 25,000 psi. This low value may create difficulty in handling iridium hardware with a thickness of <30 mil.
2. The elongation of iridium increases almost linearly with temperature up to 1093°C. This result suggests that, in terms of tensile elongation, there is no well-defined DBTT for iridium. The elongation remains at a constant value of ~40% above 1093°C.
3. In contrast, the reduction in area, which has a low value at low temperatures, increases significantly at temperatures above 500°C. This result is quite consistent with that reported by Douglass *et al.*³
4. The fracture surface shows a transition of fracture mode in iridium. Iridium fractured in a brittle manner (probably grain boundary separation) at and below 500°C and in a ductile manner at and above 760°C. Thus, there is a correlation between reduction in area and the fracture mode.

Table 13. Tensile Properties of Commercial Iridium
Recrystallized 1 Hr at 1500°C^a

Testing Temperature (°C)	Tensile Strength (psi)	Yield Strength (psi)	Elongation (%)	Reduction in Area (%)	Fracture Mode
Room	56,000	25,000	5.7	6.5	Brittle
400	77,000	17,000	15	10	Brittle
500	72,700	22,000	14.7	11	Brittle
760	56,000	21,000	23.5	24	Ductile
1093	35,000	16,000	39.6	>60	Ductile
1316	26,000	13,000	38	>60	Ductile

^a0.020-in. sheet, strain rate 0.05 in./in./min.

In order to produce polycrystalline iridium from zone-refined stock, a bar specimen was strained 20% at 800°C, followed by annealing at 1600°C. Preliminary results show that fine-grained iridium cannot be produced by repetition of this strain-annealing process.

To show the effect of a heat pulse as during re-entry of the MHW heat source on the tensile properties of iridium, sheet specimens were heated 5 min in vacuum after recrystallization for 1 hr at 1500°C. The tensile results obtained to date at various temperatures are presented in Table 14. Except for the one test which gives a low elongation of 6.4% at 1093°C, the data in the table indicate that both tensile strength and ductility are insensitive to the heat-pulse treatment, although the yield strength is considerably lower than the as-recrystallized data shown in Table 13. A plot of elongation as a function of temperature shows no well-defined ductile-to-brittle transition temperature in iridium.

Table 14. Tensile Properties^a of Commercial Iridium^b Annealed 5 Min at 2000°C after Recrystallization for 1 Hr at 1500°C

Testing Temperature (°C)	Yield Strength (psi)	Tensile Strength (psi)	Elongation (%)
Room	11,500	46,100	8.5
500	17,800	61,200	17.8
760	11,500	57,000	24.3
1093	8,500	32,000	36.2
1093	9,000	13,500	6.4
1316	10,500	23,000	33.7

^aTested in vacuum.

^b0.020-in.-thick sheet, strain rate 0.05 in./in./min, 1-in. gage length.

PHYSICAL METALLURGY OF REFRACTORY ALLOYS

(Division of Reactor Development and Technology Program 04 40 02 05 1)

C. T. Liu
Metals and Ceramics Division

Effect of Oxygen Contamination on the Mechanical Properties of Molybdenum-Base Alloys

Previous work indicates that TZM is compatible with low-pressure oxygen and CO at 825°C (Pioneer operation temperature). In order to further evaluate TZM for space isotopic heat sources at higher temperatures, a series of sheet specimens was doped with oxygen at 1×10^{-5} torr oxygen pressure and at 1000°C for different periods of time. Table 15 summarizes the tensile results obtained at room and elevated temperatures. TZM shows

Table 15. Tensile Properties of 20-mil-thick TZM Sheet Specimens Doped with Oxygen at 1×10^{-5} Torr at 1000°C and Tested at Various Temperatures

Doping Time (hr)	Oxygen ^a Content (ppm)	Elongation (%)	Yield Strength (psi)	Tensile Strength (psi)
<u>Room Temperature</u>				
0 ^b	19	37.0	61,000	79,000
0 ^b	22	33.5	62,000	79,600
25	160	17.8	66,700	83,000
50	220	5.7	72,800	83,500
96	310	0.5 ^c	—	86,200
207	480	0.5 ^c	—	57,000
<u>825°C</u>				
0 ^b		24.8	20,000	45,000
25		15.4	30,000	46,300
50		12.0	35,000	48,800
96		6.7	43,000	54,000
207		2.5	71,500	63,000
<u>1093°C</u>				
0 ^b		23.0	28,000	38,000
25		12.8	29,000	38,000
50		6.5	34,000	38,500
96		3.2	39,000	40,200
207		0.7	48,100	48,100
<u>1316°C</u>				
0		30.0 ^d	—	22,000 ^d
25		8.0	26,000	28,700
50		6.3	25,700	28,000
207		0.5 ^c	—	31,300

^aOxygen content obtained from vacuum fusion analysis. No apparent change of carbon, nitrogen, and hydrogen content.

^bRecrystallized 1 hr at 1500°C.

^cFractured within elastic limit.

^dData collected from General Electric, *Multi-Hundred Watt, Radioisotope Thermoelectric Generator Program*, GES-7034 (March 1970).

a sharp increase of yield strength with doping time. The yield strength at 825°C increases by a factor of 3 after 207 hr of exposure. Comparatively, the tensile strength is less sensitive to the oxygen contamination. The ductility decreases sharply with doping time, and TZM is completely brittle at all temperatures within a 200-hr exposure. Like oxygen-contaminated T-111, an increase in the testing temperature does not significantly improve the ductility. Note that TZM, like T-111, is also less sensitive to the oxygen contamination when tested at 825°C. Based on the data in the table, we conclude that TZM is not compatible with low-pressure oxygen at 1000°C.

Effect of Carbon Monoxide Contamination on the Mechanical Properties of Molybdenum-Base Alloys

TZM specimens were exposed to 1×10^{-5} torr CO at 1000°C for different periods of time to determine in simulation its compatibility with gases outgassed from graphite and Min-K 1301. The results of tensile tests are presented in Table 16. The tensile strength shows a general increase

Table 16. Tensile Properties of 20-mil-thick TZM Sheet Specimens Contaminated with CO at 1×10^{-5} Torr and 1000°C and Tested at Various Temperatures

Doping Time (hr)	Elongation (%)	Tensile Strength (psi)
<u>Room Temperature</u>		
0	37	79,000
240	37.3	80,500
500	3.9	80,000
1000	1.1	83,800
<u>825°C</u>		
0	24.8	45,000
1000	15.3	50,700
<u>1093°C</u>		
0	24 ^a	33,000 ^a
1000	3.2	40,800
<u>1316°C</u>		
0	30 ^a	22,000
240	29	28,000
500	29.7	27,000

^aData collected from General Electric, *Multi-Hundred Watt, Radioisotope Thermoelectric Generator Program*, GES-7034 (March 1970).

with doping time. The ductility at room temperature drops sharply between 240- and 500-hr exposures at 1000°C but remains constant at a value of approximately 30% at 1316°C. As shown in Table 16, the ductility after 1000 hr of exposure is a maximum at 825°C. TZM doped with CO behaves quite differently from that doped in oxygen. Complete characterization requires more data.

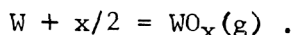
MATERIALS COMPATIBILITY TESTING FOR THE LASL-DART PROJECT

J. R. DiStefano and A. C. Schaffhauser
Metals and Ceramics Division

Compatibility couples involving several non-fuel materials being considered in constructing the DART were examined after 500 hr at 1300, 1400, and 1500°C, and the data are summarized in Tables 17-19. Only the couples tested at 1400°C were examined in detail.

From the data it would appear that graphite is very compatible with BeO, W, Re, and Pt-Rh-W up to 1500°C. In cases where tungsten and rhenium cracked, it did not appear to be the result of interaction with the graphite and probably occurred during cutting and/or mounting.

All three oxides, ZrO₂, HfO₂, and BeO, showed good compatibility with the metals they were tested against. Visual observation indicated some discoloration of both ZrO₂ and HfO₂, and relatively large weight losses were noted in both those oxides. Beryllium oxide showed little tendency to interact even in the 1500°C tests that were examined. However, a rather serious mass transfer effect was found in the closed tungsten capsule that contained BeO. The tungsten showed rather large weight losses and had an etched appearance indicative of dissolution. Since this was not observed in the couple that was tested in dynamic vacuum, it seems likely that oxygen was involved in the process. One possible type of reaction is



The source of oxygen is the BeO, and for vapor transport to occur, the reverse reaction must take place somewhere in the system. The driving force for the reverse reaction is difficult to postulate. An activity gradient could occur from a temperature gradient, pressure change, or energy change as a result of geometrical considerations. For a closed system of the type we have, it is hard to identify the reason for such an energy gradient to occur. However, we previously found the same type of thing when we exposed tungsten to Cm₂O₃.⁴

Table 17. Summary of 1400°C Compatibility Test Data for LASL-DART Project

Sample No.	Couple	Visual Observation	Metallographic Observations	Chemical Analysis (wt %)		Hardness
				Carbon in Metal	Oxygen in Metal	
1B	C-Ta	R,S	Two layers on Ta surface to depth of 3 mils	0.024		Matrix = 112 DPH Layer = 1512 DPH
2B	C-W	NR	No interaction	0.0017		Matrix = 375 DPH
3B	C-Mo	R,D,S	Reaction zone in Mo to 27 mils deep	0.050		Matrix = 151 DPH Layer = 1100 DPH
4B	C-BeO	D	No interaction	0.020		
5B	C-Re	S	Re cracked; no surface reaction zone, but Re either heavily twinned or contains needle-like precipitates throughout	0.012		Matrix = 381 DPH
6B	C-(Mo-50% Re)	R,S,D	Reaction zone in Mo-50% Re to 56 mils			Matrix = 343 DPH Layer = 1390 DPH
7B	C-(Pt-Rh-W)	R,S,D	Specimen joined to graphite, but no reaction zone; surface of Pt-Rh-W slightly roughened	0.02-1.03 ^a		Matrix = 235 DPH
Mo-2	Mo-ZrO ₂	F,C	No interaction		0.0059	
W-2	W-ZrO ₂	F,C	No interaction		0.0008	
Ta-2	Ta-ZrO ₂	F,C	No interaction		0.0280	
Mo-5	Mo-HfO ₂	F,C,SR	No interaction		0.0130	
W-5	W-HfO ₂	C	No interaction		0.0014	
Ta-5	Ta-HfO ₂	F,C	Very slight (<0.1 mil) surface reaction		0.0300	
Mo-8	Mo-BeO	NR	No interaction		0.0074	
Mo-11	Mo-BeO	NR	No interaction		0.0062	
W-8	W-BeO	NR	Slight surface roughness		0.0012	
W-11	W-BeO	NR ^b	Slight surface roughness		0.0006	
Re-1	Re-BeO	NR	Re surface irregular structure either shows a Widmanstatten second phase precipitate or is very highly twinned		<0.0001	
(Mo-50 Re)-1	(Mo-50% Re)-BeO	NR	Chain-like grain-boundary precipitate throughout Mo-50% Re		0.0040	
Mo-14	Mo-Re	S	Three distinct layers in diffusion zone; some voids in Mo-rich layer			
W-14	W-Re	S	Samples parted when cut; Re surface rough; layer on W surface; some voids in W			
W-17	W-(Mo-50% Re)	NR	Chain-like grain-boundary phase throughout Mo-50% Re			
(Mo-50 Re)-3	(Mo-50% Re)-Ir	D	Chain-like grain-boundary phase throughout Mo-50% Re			

^aSome graphite stuck to surface of specimen.^bTungsten has etched appearance.

R = visible reaction

S = couple stuck together

SR = slight reaction

C = ceramic discolored

D = surface of specimen discolored

NR = no visible reaction

F = ceramic flaked, chipped, or cracked

Table 18. Summary of 1500°C Compatibility Test Data for LASL-DART Project

Sample No.	Couple	Visual Observation	Metallographic Observations	Chemical Analysis ^a (wt %)
1C	C-Ta	S,R,D		
2C	C-W	S,R	W cracked (probably during cutting); slight surface roughening	
3C	C-Mo	S,R,D		
4C	C-BeO	R,D	No reaction	0.044
5C	C-Re	S	Re badly cracked, but there was no evidence of reaction	0.380
6C	C-(Mo-50% Re)	S,D		
7C	C-(Pt-Rh-W)	S,R,D	Reaction to depth of ~1 mil	0.056
Mo-3	Mo-ZrO ₂	C,F,NR		
W-3	W-ZrO ₂	C,F,NR		
Ta-3	Ta-ZrO ₂	C,S		
Mo-6	Mo-HfO ₂	C,F,SR		
W-6	W-HfO ₂	C,NR		
Ta-6	Ta-HfO ₂	C,SR		
Mo-9	Mo-BeO	NR	No reaction	
Mo-12	Mo-BeO	NR		
W-9	W-BeO	NR		
W-12	W-BeO	b	No reaction	
Re-2	Re-BeO	NR	Slight surface roughening; high degree of twinning or deformation lines in microstructure	
(Mo-50 Re)-2	(Mo-50% Re)-BeO	NR	Slight surface roughening	
Mo-15	Mo-Re	S		
W-15	W-Re	S		
(Mo-50 Re)-4	(Mo-50% Re)-Ir	R		

^aCarbon in metal.^bTungsten has etched appearance.

R = visible reaction

S = couple stuck together

SR = slight reaction

C = ceramic discolored

D = surface of specimen discolored

NR = no visible reaction

F = ceramic flaked, chipped, or cracked

Table 19. Summary of Weight Change Data on Compatibility Couples

Couple	Weight Change (mg)					
	1300°C		1400°C		1500°C	
	C	Metal	C	Metal	C	Metal
C-Ta	a	a	a	a	-4.1	+15.4
C-W	-0.7	0	-0.7	0	-2.2	+9.4
C-Mo	-7.7	+13.5	a	a	-1.2	-58.6
C-BeO	+0.6	-2.3	-	-3.6	-5.6	-75.7
C-Re	a	a	a	a	a	a
C-(Mo-50% Re)	a	a	-19	+38.7	a	a
C-(Pt-Rh-W)	-1.2	+2.0	a	a	a	a
	Oxide	Metal	Oxide	Metal	Oxide	Metal
Mo-ZrO ₂	b	b	-10.6	0	b	b
W-ZrO ₂	b	b	-70.5	+3.0	b	b
Ta-ZrO ₂	b	b	-41.8	+1.4	b	b
Mo-HfO ₂	b	b	-116	+8.3	b	b
W-HfO ₂	b	b	-11.9	+5.0	b	b
Ta-HfO ₂	b	b	-60.0	+2.5	b	b
Mo-BeO	b	b	-5.5	0	-6.0	-0.2
Mo-BeO ^C	b	b	-2.6	0	b	b
W-BeO	b	b	-4.6	+7.0	b	b
W-BeO ^C	b	b	0	-2.5	-1.9	-610
Re-BeO	b	b	-4.1	+1.5	-4.0	0
(Mo-50% Re)-BeO	b	b	-4.1	+1.0	-5.7	+4.2
	Metal 1	Metal 2	Metal 1	Metal 2	Metal 1	Metal 2
Mo ¹ -Re ²	b	b	0	d	b	b
W ¹ -Re ²	b	b	-1.5	d	b	b
W ¹ -(Mo-50% Re) ²	b	b	0	+1.2	b	b
(Mo-50% Re) ¹ -Ir ²	b	b	+4.8	-6.8	+3.4	-5.1

^aGraphite stuck to metal

^bSample not weighed.

^cClosed capsule.

^dSample stuck to sample holder.

REFERENCES

1. Eugene Lamb and R. G. Donnelly, *ORNL Isotopic Power Fuels Quarterly Report for Period Ending March 31, 1972*, ORNL-4796, Oak Ridge National Laboratory.
2. General Electric Company, *Multi-Hundred Watt, Radioisotope Thermo-electric Generator Program for Period from October 1, 1971, to December 31, 1971*.
3. R. W. Douglass *et al.*, *High Temperature Properties and Alloying Behavior of the Refractory Platinum Group Metals*, NP-10939, Battelle Memorial Institute (August 1961).
4. J. R. DiStefano and K. H. Lin, *Compatibility of Curium Oxide with Refractory Metals at 1650°C and 1850°C*, ORNL-4773, Oak Ridge National Laboratory (March 1972), pp. 21-36.

3

ORNL-4814
UC-33 - Propulsion Systems and
Energy Conversion

INTERNAL DISTRIBUTION

- | | | | |
|-------|-------------------------------|--------|-------------------------------|
| 1-3. | Central Research Library | 38. | Lynda Kern |
| 4. | ORNL - Y-12 Technical Library | 39. | E. Lamb |
| | Document Reference Section | 40. | R. E. Leuze |
| 5-24. | Laboratory Records Department | 41. | H. C. McCurdy |
| 25. | Laboratory Records, ORNL R.C. | 42. | R. E. McHenry |
| 26. | G. M. Adamson, Jr. | 43-44. | R. A. Robinson |
| 27. | T. A. Butler | 45. | A. F. Rupp |
| 28. | W. R. Casto | 46. | R. W. Schaich |
| 29. | F. L. Culler | 47. | M. J. Skinner |
| 30. | J. E. Cunningham | 48. | A. H. Snell |
| 31. | R. G. Donnelly | 49. | D. A. Sundberg |
| 32. | D. E. Ferguson | 50. | D. B. Trauger |
| 33. | J. H. Frye, Jr. | 51. | A. M. Weinberg |
| 34. | J. H. Gillette | 52. | C. M. Adams, Jr. (consultant) |
| 35. | R. F. Hibbs | 53. | Walter Kohn (consultant) |
| 36. | M. R. Hill | 54. | Sidney Siegel (consultant) |
| 37. | H. Inouye | | |

EXTERNAL DISTRIBUTION

55. R. D. Baker, Los Alamos Scientific Laboratory
56. R. T. Carpenter, Division of Space Nuclear Systems, AEC
57. W. T. Cave, Mound Laboratory
58. Commander, Naval Undersea Research and Development Center
59. G. R. Crane, Headquarters AFSC (XRTS), Andrews Air Force Base
60. D. P. Davis, Dayton Area Office, AEC
61. G. P. Dix, Division of Space Nuclear Systems, AEC
62. R. K. Flitcraft, Mound Laboratory
- 63-65. E. E. Fowler, Division of Applied Technology, AEC
66. D. S. Gabriel, Division of Space Nuclear Systems, AEC
67. N. Goldenberg, Division of Space Nuclear Systems, AEC
68. G. L. Hagey, Naval Facilities Engineering Command
69. R. C. Hamilton, IDA - Room 19, 400 Army-Navy Drive, Arlington, Va.
70. R. E. Hopkins, U.S. Army Mobility Equipment R&D Center
71. T. B. Kerr, NASA Headquarters
72. F. E. Kruesi, Savannah River Laboratory
73. J. A. Lieberman, Division of Reactor Development and Technology, AEC
74. W. A. McDonald, Isotopes, Inc.
75. T. A. Nemzek, Richland Operations Office, AEC
76. G. A. Newby, Division of Space Nuclear Systems, AEC
77. J. A. Powers, Division of Space Nuclear Systems, AEC
78. R. Schafer, General Electric Company
79. S. J. Seiken, Division of Reactor Development and Technology, AEC
80. M. Shaw, Division of Reactor Development and Technology, AEC
81. J. A. Swartout, Union Carbide Corporation
82. Director, Pacific Northwest Laboratory

83. AEC, Savannah River Operations Office
84. General Electric Company, MSD, AEC
85. General Electric Company, VNC, AEC
86. Isotopes, Inc., Middle River, AEC
87. NASA, Goddard Space Flight Center
88. NASA, Langley Research Center
89. NASA, Manned Spacecraft Center
90. NASA, Marshall Space Flight Center
91. Navy Space Systems Activity
92. Radio Corporation of America, AEC
93. Thermo Electron Corporation, AEC
94. Research and Technical Support Division, AEC-ORO
95. Patent Office, AEC-ORO
- 96-269. Given distribution as shown in TID-4500 (59th ed.) under Propulsion Systems and Energy Conversion category (25 copies - NTIS)